High-resolution optical spectroscopy investigation of Nd_2BaNiO_5 and $Nd_{0.1}Y_{1.9}BaNiO_5$ and crystal-field parameters for rare-earth linear-chain nickelates

M. N. Popova,* S. A. Klimin, E. P. Chukalina, and E. A. Romanov
Institute of Spectroscopy, Russian Academy of Sciences, 142190 Troitsk, Moscow region, Russia

B. Z. Malkin
Kazan State University, 420008 Kazan, Russia

E. Antic-Fidancev
Laboratoire de Chimie Appliquée de l'État Solide, CNRS-UMR7574, ENSCP, 11, Rue Pierre et Marie Curie, F-75231 Paris Cedex 05, France

B. V. Mill
Moscow State University, Physics Department, 119899 Moscow, Russia

G. Dhalenne
Laboratoire de Physico-Chimie de l'État Solide, Université Paris-Sud, F-91405 Orsay, France
(Received 27 July 2004; revised manuscript received 3 November 2004; published 19 January 2005)

High-resolution spectroscopy of Nd^{3+} in Nd_2BaNiO_5 and Y_2BaNiO_5:Nd(5%) powder samples is used to study Nd^{3+} crystal-field levels and exchange splittings in these quasi-one-dimensional model compounds. We demonstrate that the Nd^{3+} ground-state splitting in the magnetically ordered state of Nd_2BaNiO_5 ($T_N = 47.5 \pm 1$ K, as found from our spectroscopic data) accounts for the low-temperature magnetic properties and for the 4-meV mode observed earlier in inelastic neutron scattering experiments. Crystal-field analysis is performed. Its results show that the directions of ordered magnetic moments in Nd_2BaNiO_5 are determined by the single-ion anisotropy of Nd^{3+}. We argue that the crystal-field parameters obtained for Nd-nickelate (in this work) and Er-nickelate (in our earlier work) can be used to predict the energy-level patterns and magnetic properties of other rare-earth linear-chain nickelates.

DOI: 10.1103/PhysRevB.71.024414 PACS number(s): 75.40.Cx, 78.30.−j, 71.70.Ch

I. INTRODUCTION

Since the theoretical work of Haldane[1] that predicted a quantum-disordered singlet ground state and an energy gap in the excitation spectrum of a one-dimensional (1D) Heisenberg antiferromagnet with integer spin, crystals containing isolated chains of magnetic Ni^{2+} ($S=1$) ions have been the object of extensive investigation. Among these, the linear-chain nickelates R_2BaNiO_5 (R=Pr-Tm, Y), due to peculiarities of their structure, appeared to be excellent model materials for studying the crossover from 1D quantum to 3D classical behavior. The chains of flattened NiO_6 octahedra running along the *a* axis of the orthorhombic structure (space group *Immm*) have no direct links between them and are interconnected through Ba^{2+} and R^{3+} ions residing in C_{2v}-symmetry positions (see, e.g., Ref. 2 and references therein and Fig. 1). While Y_2BaNiO_5 of this family does not order magnetically, at least down to 100 mK,[3] and exhibits the Haldane gap $\Delta_H \approx 80$ cm^{-1},[4] the replacement of yttrium with a magnetic rare earth results in 3D antiferromagnetic (AF) order at T_N ranging from 12.5 K for Tm_2BaNiO_5 to 65 K for Tb_2BaNiO_5.[5–7] By preparing samples with different proportions of nonmagnetic yttrium and magnetic rare earths, it is possible to smoothly change T_N.

Such a mixed system with Nd, $(Nd_xY_{1-x})_2BaNiO_5$, was recently used to study, by the inelastic neutron scattering

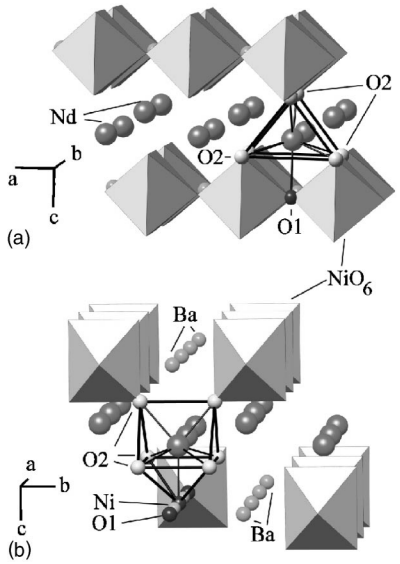

FIG. 1. Fragment of the Nd_2BaNiO_5 structure in two crystallographic projections (a) and (b). The chains of NiO_6 octahedra are shown. The chains are connected via NdO_7 capped prisms. Two crystallographic types of oxygen in Nd^{3+} surrounding (six O_2 and one O_1) are discussed in the text. Two octahedra in the (b) picture are deleted to clarify connection of the NdO_7 polyhedron to the Ni—O—Ni chain.

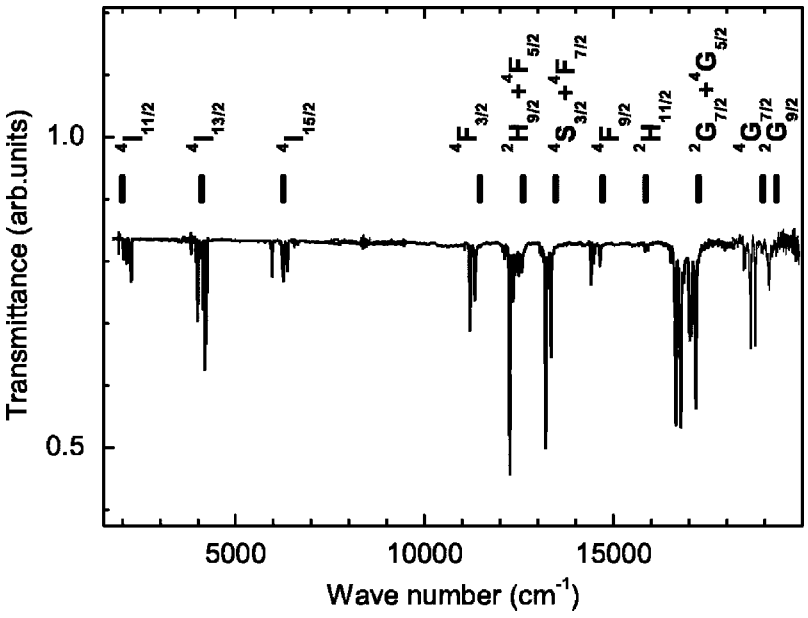

FIG. 2. Diffuse transmittance spectrum of paramagnetic Nd_2BaNiO_5 at ~100 K. Positions of CF manifolds in $LaCl_3:Nd^{3+}$ (Ref. 14) are indicated on the top.

technique, the crossover from a 1D quantum singlet ground state to 3D classical Néel ground state and the behavior of the Haldane gap through 1D to 3D crossover.[8–10] The Haldane-gap excitations of nickel chains were found to coexist with long-range AF order. Another neutron experiment (on Nd_2BaNiO_5) revealed a substantial interference between the 1D Haldane-gap excitations of Ni^{2+} chains and a local crystal-field (CF) level of Nd^{3+}.[11] The observed phenomenon was qualitatively described by a simple random-phase-approximation model for $Ni^{2+}-R^{3+}$ interactions. A quantitative theory was prevented by a lack of information on the electronic states of the Nd^{3+} ions.[11]

Such an information is also necessary to explain the magnetic properties of Nd_2BaNiO_5: namely, why the magnetic susceptibility $\chi(T)$ has a maximum at the temperature $T_{max}=26$ K (Ref. 12) (30 K, according to Ref. 5), much lower than $T_N \approx 48$ K (Refs. 6 and 7) (46.5 K, according to Ref. 5). The neutron data showed that there is no magnetic symmetry change at T_{max}. Probably, the maximum in the magnetic susceptibility versus temperature curve, $\chi(T)$, is caused by a depopulation of the upper component of the ground Kramers doublet of Nd^{3+} split in the magnetically ordered state, analogously to the case of Er_2BaNiO_5.[5,13] To confirm this hypothesis, spectroscopic measurements are necessary.

Thus, knowledge of the CF levels and their splitting in the magnetically ordered state, CF parameters, and wave functions for Nd^{3+} in Nd_2BaNiO_5 chain nickelate is of primary importance for a deeper understanding of the magnetic and dynamic properties of this quasi-1D quantum antiferromagnet. Up until now, only the lowest-energy CF excitations with the energy 144, 192, and 304 cm^{-1} have been reported from the measured inelastic neutron scattering spectra.[11] The absence of any optical spectroscopic information can be explained by difficulties in registering spectra of this opaque compound. In the present work, we overcome these difficulties by using the advantages of Fourier-transform spectroscopy and our special technique for powder samples.

We report the results of a high-resolution (0.1 cm^{-1}) spectral study of the optical transitions between the CF levels of the ground $^4I_{9/2}$ and excited manifolds of Nd^{3+} in Nd_2BaNiO_5 and in $Y_2BaNiO_5:Nd$ (used for a comparison). The positions of CF levels in a broad energy range and their exchange splittings in the magnetically ordered state of Nd_2BaNiO_5 are measured directly. We discuss the influence of the observed Nd^{3+} ground-state splitting over the magnetic and dynamic properties of Nd_2BaNiO_5. We perform the crystal-field analysis, find nine CF parameters for Nd^{3+} ($4f^3$) in Nd_2BaNiO_5, and compare them to those obtained earlier for Er^{3+} ($4f^{11}$) in Er_2BaNiO_5.[13] Further, we estimate the CF parameters for other R^{3+} ($4f^n$) ions in R_2BaNiO_5 using the linear interpolation (in the number n of $4f$ electrons) and show that they describe well the experimental data available from literature and, thus, can be used to predict the energy levels and magnetic properties of these linear-chain model compounds.

II. RESULTS AND DISCUSSION

A. Optical spectra of Nd_2BaNiO_5 and $Nd_{0.1}Y_{1.9}BaNiO_5$ in the paramagnetic state and crystal-field levels of Nd^{3+}

The polycrystalline Nd_2BaNiO_5 and $Nd_{0.1}Y_{1.9}BaNiO_5$ samples for optical studies were prepared using the procedure similar to the one described in our previous paper.[13] High-resolution (up to 0.1 cm^{-1}) diffuse transmittance spectral measurements in a broad range of frequencies (1600–20 000 cm^{-1}) and temperatures (2.5–300 K) were performed on a Fourier-transform spectrometer BOMEM DA3.002.

Figure 2 shows the transmission of the Nd_2BaNiO_5 powder sample in the whole spectral region studied. Sharp lines are due to *f-f* electronic transitions within the Nd^{3+} ions, from the ground $^4I_{9/2}$ CF manifold to a series of excited manifolds. For a comparison, sticks on the top of the spectrum show the positions of CF manifolds of Nd^{3+} in $LaCl_3$.[14] While the crystal field levels of the low-lying Nd^{3+} multiplets $^4I_{11/2}$, $^4I_{13/2}$, and $^4I_{15/2}$ are in the same energy intervals for both Nd_2BaNiO_5 and LaF_3, higher-energy crystal-field

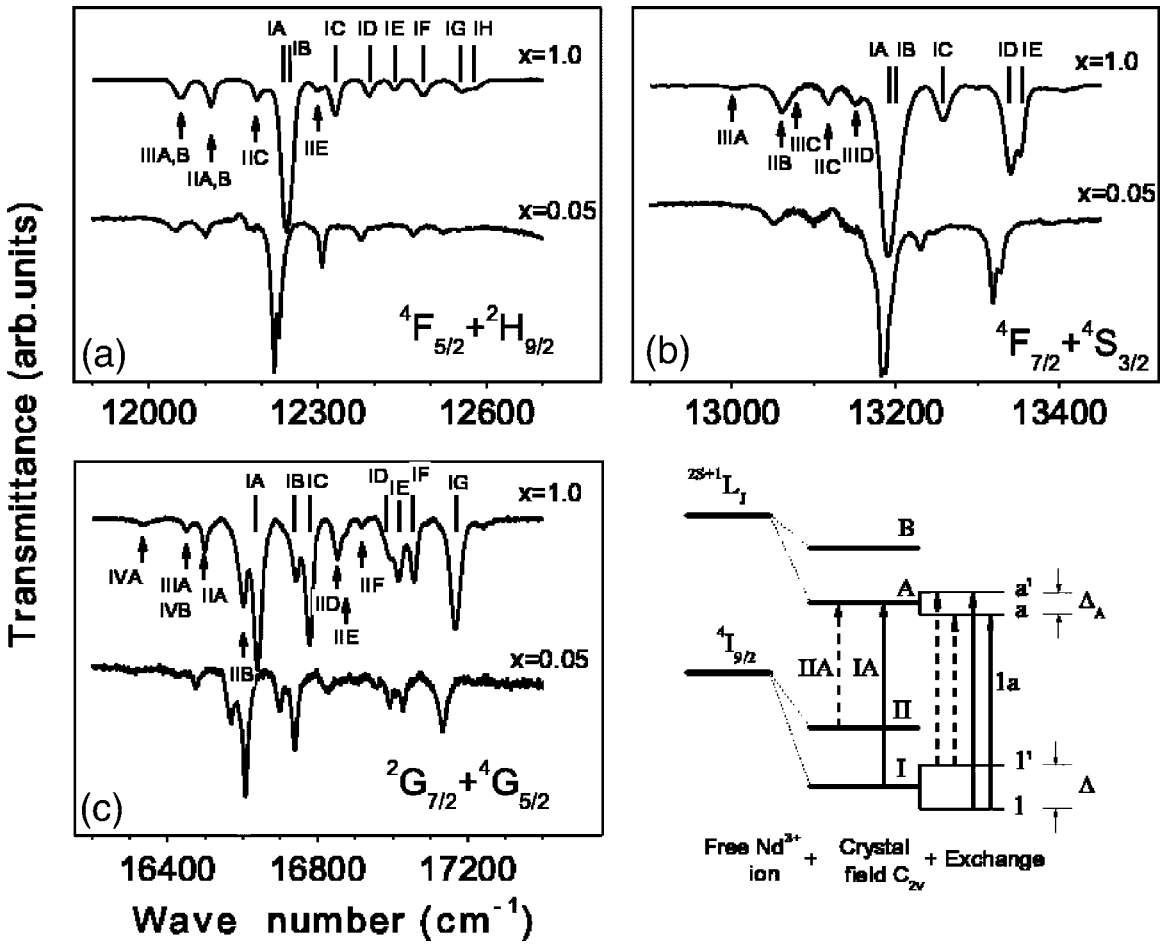

FIG. 3. Spectra due to transitions from the ground $^4I_{9/2}$ level to several excited levels (indicated in the lowest right corner of each frame) in $(Nd_xY_{1-x})_2BaNiO_5$ at $T=100$ K. Spectral lines are marked in accordance with the presented scheme.

manifolds for Nd_2BaNiO_5 are shifted to the low-energy side in comparison with their position in $LaF_3:Nd^{3+}$. This nephelauxetic shift[15–17] is due to a greater overlap of Nd^{3+} excited-state wave functions with ligand wave functions in Nd_2BaNiO_5.

In a crystal field of local C_{2v} symmetry each free-ion Nd^{3+} level characterized by the momentum J splits into $J+1/2$ Kramers doublets (see the scheme of Fig. 3). All spectra could be analyzed in terms of a single Nd^{3+} site. To facilitate the analysis, we used spectra of the diluted compound $Nd_{0.1}Y_{1.9}BaNiO_5$ that does not order magnetically down to at least 10 K and, hence, the spectral pattern is not complicated by exchange splittings. The spectra of both compounds are compared in Fig. 3 for several selected multiplets. Such a comparison allowed us to resolve several closely lying crystal-field levels [see, e.g., CF doublets *IA-IB* in Figs. 3(a) and 3(b)]. The general appearance of the spectra is similar for both compounds but the spectral lines are shifted, in contrast to the case of the $(Er_xY_{1-x})_2BaNiO_5$ system where the positions of spectral lines are independent of x.[13] This is due to the appreciably greater difference in the ionic radii between Nd^{3+} ($r=0.098$ nm) and Y^{3+} ($r=0.090$ nm) than between Er^{3+} ($r=0.089$ nm) and Y^{3+}. The energies of the CF levels found from the spectra are presented in Table I. The CF levels of the ground $^4I_{9/2}$ manifold were determined from the spectra at elevated temperatures, taking into account the temperature behavior of corresponding spectral lines. We checked that the intensities of the lines which inflamed with increasing the temperature correlate with the populations of the corresponding excited CF sublevels. The positions of the three lowest-lying levels as determined from optical spectroscopy (140, 190, and 302 cm^{-1}) are in agreement with the positions found from inelastic neutron scattering data [144, 192, and 304 cm^{-1} (Ref. 11)].

B. Crystal-field calculations

To fit parameters of the CF Hamiltonian [see Eq. (3) in Ref. [13]] to the observed values of level energies, it is desirable to have an initial set of CF parameters found from a reasonable physical model for the crystal field. We use here the exchange-charge model (ECM), which takes into account the contributions from both the exchange interactions with the nearest neighbors and the field of point charges (PC's) at the regular lattice sites.[18] A detailed description of the application of the ECM to the case of R_2BaNiO_5 is given in Ref. 13. As in the case of Er_2BaNiO_5,[13] we use different model parameters (i.e., phenomenological scaling factors G_σ and G_π, which determine exchange charges at the σ and π bonds, respectively) in calculations of contributions into CF param-

TABLE I. Experimentally measured at 90 K (E_{expt}) and calculated (E_{calc}) crystal-field energies in $Nd_{2x}Y_{2(1-x)}BaNiO_5$. Exchange splittings of Kramers doublet states at 5 K (in cm^{-1}) are in parentheses.

	E_{expt} (cm^{-1})		E_{calc} (cm^{-1})
Multiplet	$x=1$	$x=0.05$	$x=1$
$^4I_{9/2}$	0 (32)	0	0
	140	130	141
	190	180	191
	302	290	296
	~440 (300 K)	440	444
$^4I_{11/2}$	1901	1909	1897
	2029	2018	2017
	2046	2040	2029
	2104	2100	2092
	2183	2178	2163
	2224	2222	2219
$^4I_{13/2}$	3807		3833
	3970	3956	3958
	3992 (11)	3978	3981
	4029	4022	4011
	4119	4117	4111
	4169	4160	4151
	4217	4212	4211
$^4I_{15/2}$	5772		5786
	5912 (16)		5913
	5956 (<4)		5966
			6025
	6163		6167
	6220		6228
	6248		6248
	6353		6349
$^4F_{3/2}$	11188 (11.4)	11182	11172
	11323	11290	11284
$^4F_{5/2}$	12241 (<2)	12222	12216
	12251 (<2)	12231	12234
	12330 (3.7)	12306	12343
$^4H(2)_{9/2}$	12390	12377	12400
	12438	12410	12445
	12490	12470	12472
	12552	12521	12543
	12580	12551	12609
$^4F_{7/2}$	13190 (5.3)	13183	13193
	13200 (5.3)	13187	13205
	13258 (4)	13229	13268
			13388
$^4S_{3/2}$	13340 (14.5)	13318	13343
	13352 (22)	13327	13352
$^4F_{9/2}$	14390 (2)	14379	14398
	14468 (7)	14447	14475

TABLE I. (*Continued.*)

	E_{expt} (cm^{-1})		E_{calc} (cm^{-1})
Multiplet	$x=1$	$x=0.05$	$x=1$
			14565
			14610
	14631 (14)	14603	14626
$^2H(2)_{11/2}$			15727
			15746
			15755
			15770
			15791
			15802
$^4G_{5/2}$	16640 (6)	16608	16635
	16743 (10)	16699	16726
	16779 (7)	16738	16808
$^2G_{7/2}$	16996	16992	17009
	17015	17026	17018
	17057		17033
	17168	17132	17173
$^4G_{7/2}$	18585	18600	18559
	18625		18623
		18704	18647
	18748		18784
$^2G_{9/2}$			18973
	19114		19100

eters from interactions of the R^{3+} ion with essentially different oxygen ions, O(1) and O(2), from the first coordination sphere [O(1) ions accomplish the shortest 180° superexchange bonds Ni-O-Ni within the nickel chains: see Fig. 1]. The ionic charges Z in Nd_2BaNiO_5 were assumed to be the same as in Er_2BaNiO_5, and the corresponding contributions to the CF parameters (see Table II, column 2) were calculated using the lattice structure parameters from Ref. 2 with the shielding constants $\sigma_2=0.8$ and $\sigma_4=\sigma_6=0$ (Ref. 19) and the moments of the radial distribution of the $4f$ electron density from Ref. 20. Each Nd^{3+} ion has seven O^{2-} ligands at distances $R\mathrm{O}(1)=0.2352$ nm, $R\mathrm{O}(2)=0.2339$ nm (two ligands), and $R\mathrm{O}(2')=0.2481$ nm (four ligands). The relevant overlap integrals ($\langle \mathrm{Nd}^{3+}4fm|\mathrm{O}^{2-}2pm\rangle, m=0,1$), calculated with the corresponding radial functions from Refs. 20 and 21, equal (in units of 10^{-2}): $S_\sigma[R\mathrm{O}(1)]=2.044$, $S_\pi[R\mathrm{O}(1)]=1.576$, $S_\sigma[R\mathrm{O}(2)]=2.0755$, $S_\pi[R\mathrm{O}(2)]=1.612$, $S_\sigma[R\mathrm{O}(2')]=1.74$, and $S_\pi[R\mathrm{O}(2')]=1.256$. The scaling factors for the exchange charges $G_\sigma[\mathrm{O}(1)]=12.8$ and $G_\sigma[\mathrm{O}(2)]=G_\sigma[\mathrm{O}(2')]=8.8$ and the general ratio $G_\pi/G_\sigma=0.875$ were found from fitting the calculated splittings of the ^4I_J multiplets to the measured splittings. Table II (column 3) summarizes the calculated CF parameters.

These parameters were used as starting values in the fitting procedure to describe the total set of CF energies presented in Table I. In this procedure we diagonalized the complete Hamiltonian of the Nd^{3+} ion determined in the basis of

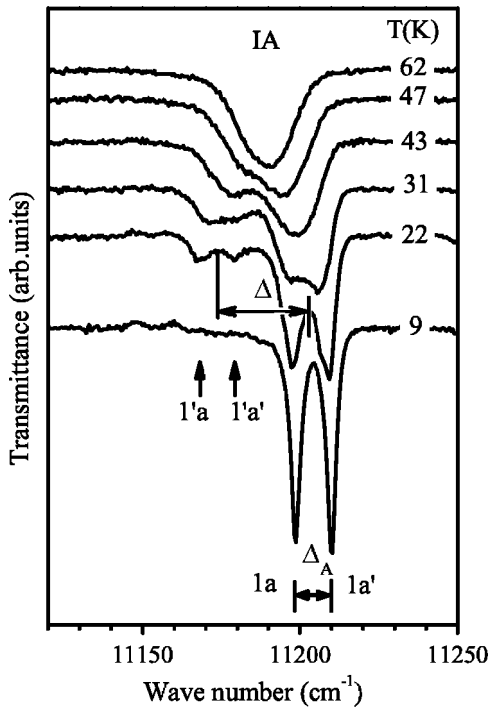

FIG. 4. The line *IA* of the transition ${}^4I_{9/2} \rightarrow {}^4F_{3/2}$ at different temperatures. Designations correspond to the scheme of Fig. 3.

364 states of the $4f^3$ configuration. Due to lack of information on energies of a number of excited multiplets, it was of no sense to vary all parameters in the Hamiltonian. Varying the electrostatic Slater parameters F^2, F^4, and F^6, Trees' parameters α and β, the constant of spin-orbit interaction ζ, and nine CF parameters and with other parameters (Trees' parameter γ, Judd three-particle parameters T^2-T^4, T^6-T^8, parameters P^k and M^k of relativistic corrections) fixed at the values known from literature,[22,23] we fitted eigenvalues of the Hamiltonian to the measured energies of 54 levels of Nd^{3+} in Nd_2BaNiO_5. The results of fitting agree fairly well

TABLE II. Crystal-field parameters B_k^p (in cm^{-1}) for R_2BaNiO_5.

		Nd_2BaNiO_5			
		Calculated			
p	k	PC	ECM	Fitted	Er_2BaNiO_5 (Ref. 13)
1		2	3	4	5
2	0	237	792	768	541
2	2	−85	−142	−221	−180
4	0	302	896	1013	706
4	2	−672	−1320	−1005	−930
4	4	−471	−920	−908	−865
6	0	74	243	210	125
6	2	−84	−154	−219	−143
6	4	90	215	232	158
6	6	−127	−305	−505	−257

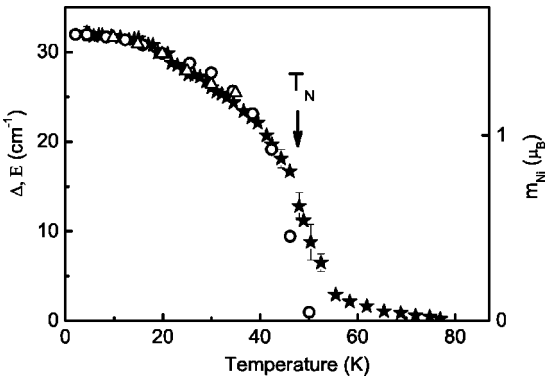

FIG. 5. Temperature-dependent Nd^{3+} ground-state spitting Δ (stars), energy E of the 4 meV excitation (open triangles), and nickel magnetic moment m_{Ni} (open circles). $\Delta(T)$ is from spectroscopic measurements of this work; $E(T)$ and $m_{Ni}(T)$ are from neutron scattering experiments (Ref. 10).

with the experimental data (see Table I). Data in the column E_{calc} were obtained with $F^2=70\,289$, $F^4=52\,220$, $F^6=34\,000$, $\zeta=871$, $\alpha=24$, $\beta=-740$, $\gamma=1688$, $T^2=236$, $T^3=44$, $T^4=60$, $T^6=-285$, $T^7=320$, $T^8=252$, $M^0=104$, $M^2=52$, $M^4=35$, $P^2=122$, $P^4=94$, and $P^6=61$ (cm^{-1}) and with the CF parameters from column 4 of Table II. The rms difference between calculated and measured CF energies equals 14.7 cm^{-1}. The obtained CF parameters correlate with those of Er_2BaNiO_5 (Table II, column 5).

The eigenfunctions of the CF states were used to calculate magnetic moments. The magnetic moment operator $\hat{\mathbf{m}}=\Sigma\mu_B(\boldsymbol{l}+2\boldsymbol{s})$ (the sum is over $4f$ electrons with orbital $\boldsymbol{l}$ and spin $\boldsymbol{s}$ moments, and μ_B is the Bohr magneton) projected on the Kramers doublet is determined by the g tensor: namely, $m_\alpha=\Sigma_\beta\mu_B g_{\alpha\beta}S_\beta$ (here $S=1/2$ is the effective spin moment). For the C_{2v} symmetry, only diagonal elements of the g tensor are different from zero. For the ground state of Nd^{3+} in Nd_2BaNiO_5 with the Kramers-conjugated wave functions $|+\rangle$ and $|-\rangle$, we obtained $g_{xx}/2=|\langle+|m_x|-\rangle|=0.17$, $g_{yy}/2=|\langle+|m_y|-\rangle|=0.48$, and $g_{zz}/2=|\langle+|m_z|+\rangle|=2.77$ (here and below magnetic moments are given in units of μ_B), in good agreement with the measured values of projections of the spontaneous Nd^{3+} moment on the crystallographic axes at 1.5 K, $m_x=-0.05$, and $m_z=2.65$.[7] The calculated values are slightly overestimated, probably due to neglect of the covalency reduction of the orbital moment. Thus, it follows from the CF calculations that the direction of the ordered magnetic moments in Nd_2BaNiO_5 is determined by the rare-earth single-ion anisotropy.

C. Exchange splittings in the spectra of Nd_2BaNiO_5

In a magnetically ordered state, magnetic interactions split the Kramers doublets of Nd^{3+} which leads to a splitting of spectral lines. A more detailed description of the method of a rare-earth probe using high-resolution Fourier-transform spectroscopy and of its possibilities in studying magnetic phase transitions can be found, e.g., in Refs. 24 and 25. Figure 4 presents an example of a line splitting in Nd_2BaNiO_5 in the course of a magnetic ordering. This is the

well-isolated line of the optical transition from the ground state to the lowest-energy level of the $^4F_{3/2}$ crystal-field doublet. One can clearly see all four components of the split line and a freezing-out of the lowest-frequency components, in accordance with the scheme of Fig. 3. Analyzing the line splittings, we were able to determine the splittings of the ground and several excited Kramers doublets. They are listed in Table I.

Figure 5 shows the temperature dependence of the ground-state splitting $\Delta(T)$ determined from the spectra, together with the temperature dependences of the energy of the 4-meV mode and of the nickel magnetic moment $m_{\mathrm{Ni}}(T)$ measured by the method of inelastic neutron scattering.[10] Figure 5 clearly demonstrates that the 4-meV mode observed in neutron scattering experiments[10,26] and first attributed to a CF transition in Nd^{3+} (Ref. 26) actually is the transition between the components of the ground Kramers doublet split by magnetic interactions in the magnetically ordered state and, thus, corresponds to a flipping of a single Nd^{3+} moment, as has been correctly suggested in Ref. 10.

For $T<0.9T_N$ the ground-state splitting is proportional to the magnetic moment of the nickel subsystem (see Fig. 5) just as for Er_2BaNiO_5.[13] In the latest case, this fact allowed us to suggest a molecular-field model to describe the magnetic behavior of erbium magnetic subsystem in an effective magnetic field B_{eff} created by the ordered nickel subsystem.[5] In the framework of this approach, one can write

$$\Delta(T) = 2m_{\mathrm{Nd}}^{(0)} B_{\mathrm{eff}}(T), \tag{1}$$

$$B_{\mathrm{eff}}(T) = \lambda m_{\mathrm{Ni}}(T). \tag{2}$$

Here $m_{\mathrm{Nd}}^{(0)}$ is the magnetic moment of a single Nd^{3+} ion in the ground state. Taking the corrected experimental data $m_{\mathrm{Nd}}^{(0)} = 2.65\mu_B$ and $m_{\mathrm{Ni}}(0) = 1.6\mu_B$ from recent neutron-scattering experiments,[7] we obtain the value $\lambda = 7.61T/\mu_B$ for the molecular-field constant from the fit of Eqs. (1) and (2) to our experimental data on $\Delta(T)$. This value is very close to the result obtained in Ref. 12 ($\lambda = 7.51T/\mu_B$) from analysis of the magnetic susceptibility of Nd_2BaNiO_5.

At $T>T_N$ the splittings of spectral lines do not vanish, exhibiting tails of residual splittings due to short-range order. Earlier, we suggested that the temperature of a magnetic ordering can be found as a point of inflection at the $\Delta(T)$ curve.[24,25] The comparison of optical and neutron scattering data on Nd_2BaNiO_5 (see Fig. 5) confirms this suggestion. Our spectroscopic data give $T_N = 47.5 \pm 1$ K, in agreement with $T_N = 48$ K communicated from neutron diffraction experiments.[6,7]

D. Determination of the ordered Nd^{3+} magnetic moment from the spectral data

The excited CF levels (140, 190 cm^{-1}, etc; see Table I) are not populated at $T<T_N$ and, thus, only the ground Kramers doublet contributes to the ordered magnetic moment (per Nd^{3+} ion) $m_{\mathrm{Nd}}(T)$ of the neodymium subsystem: namely,

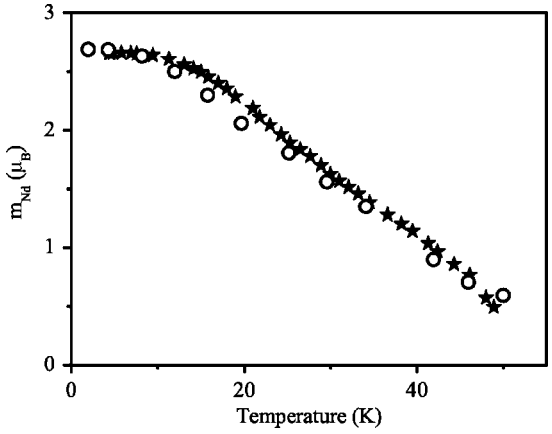

FIG. 6. Temperature dependence of the magnetic moment of the Nd^{3+} ion in the magnetically ordered phase obtained from spectral data according to Eq. (3), in comparison with neutron diffraction data (Ref. 10) (circles).

$$m_{\mathrm{Nd}}(T) = m_{\mathrm{Nd}}^{(0)} \frac{n_1 - n_2}{n_1 + n_2} = m_{\mathrm{Nd}}^{(0)} \tanh \frac{\Delta(T)}{2kT}. \tag{3}$$

Here n_1 and $n_2 = n_1 \exp(-\Delta/kT)$ are the populations of the lower and upper components of the ground Kramers doublet split by the magnetic interactions in the magnetically ordered state, respectively.

Figure 6 presents the dependence $m_{\mathrm{Nd}}(T)$ calculated with the help of Eq. (3) using spectroscopically measured exchange splittings $\Delta(T)$. A good agreement with neutron diffraction data (also presented in Fig. 6) is seen. Thus, just the Nd^{3+} ground-state exchange splitting accounts for the low-temperature behavior of the rare-earth magnetic moment in Nd_2BaNiO_5.

Our spectroscopic measurements justify an approach first suggested in Ref. 5 and used in Ref. 12 to calculate the magnetic susceptibility $\chi(T)$ of Nd_2BaNiO_5 and clearly show that the observed maximum of $\chi(T)$ at $T_{\max} \approx 26$ K is connected with a depopulation of the upper component of the Nd^{3+} ground Kramers doublet split by the Nd-Ni exchange interaction.

III. CRYSTAL-FIELD LEVELS AND MAGNETIC PROPERTIES OF OTHER RARE-EARTH LINEAR-CHAIN NICKELATES

As a rule, the CF parameters in crystals with the same chemical content and structure but with different rare-earth sublattices change monotonically with the number n of electrons at the open $4f^n$ shell. The information about CF parameters for the Nd^{3+} ($4f^3$) ions and for the Er^{3+} ($4f^{11}$) ions obtained in this work and in our earlier study[13] opens the possibility to predict the energy-level patterns and magnetic properties of rare-earth ions in different rare-earth chain nickelates from the CF calculations and to additionally check results of the CF analysis presented above.

The CF parameters for Pr^{3+} ($4f^2$), Tb^{3+} ($4f^8$), Dy^{3+} ($4f^9$), Ho^{3+} ($4f^{10}$), and Tm^{3+} ($4f^{12}$) ions were estimated using the

interpolation (linear in the number n of $4f$ electrons) between the values given in Table II (columns 4 and 5) for the Nd^{3+} ($4f^3$) and Er^{3+} ($4f^{11}$) ions. The CF Hamiltonian for the corresponding rare-earth ion (R^{3+}) was diagonalized in the space of states of the ground multiplet, and the eigenvectors were used to calculate matrix elements of the magnetic moment $\hat{\boldsymbol{m}}=\mu_B g_J \boldsymbol{J}$ (g_J is the Lande factor). Below, the results of these calculations are briefly discussed and compared to the published experimental data.

We have to note that the energy spectra of non-Kramers ions with an even number of $4f$ electrons in the CF of C_{2v} symmetry consist of singlets only. When a gap δ between the two lower singlets is much less than the energy of higher-lying CF sublevels, we consider this quasidoublet with the wave functions $|1\rangle$ and $|2\rangle$ as the ground state. In this state, the induced magnetic moment can be aligned along one of the three crystallographic axes only, and the temperature dependence of the magnetic moment in the magnetically ordered phase in the framework of mean-field approximation is determined by the expression

$$m_{\alpha R}=\frac{g_\alpha \mu_B}{2}\frac{\mu_B g_\alpha \lambda m_{\mathrm{Ni}}}{[\delta^2+(\mu_B g_\alpha \lambda m_{\mathrm{Ni}})^2]^{1/2}} \times \tanh\left\{\frac{[\delta^2+(\mu_B g_\alpha \lambda m_{\mathrm{Ni}})^2]^{1/2}}{2kT}\right\}, \quad (4)$$

where $g_\alpha=2g_J|\langle 1|J_\alpha|2\rangle|$ and λ is the same molecular-field constant as in Eq. (2) that determines the effective magnetic field at the R^{3+} ion due to exchange interactions with Ni^{2+} ions. The spontaneous magnetic moment of the nickel ion m_{Ni} may be considered nearly constant at temperatures well below T_N.

Dy_2BaNiO_5. According to the calculations, the ground state of the Dy^{3+} ion is a well-isolated Kramers doublet (the next CF sublevel of the $^6H_{15/2}$ multiplet is lying more than 120 cm^{-1} higher). The calculated nonzero matrix elements of the magnetic moment in the ground state, $g_{xx}/2=0.08$, $g_{yy}/2=0.04$, and $g_{zz}/2=9.66$, agree qualitatively with the measured components of the ordered magnetic moment at 1.5 K, $m_x=0.06$ and $m_z=7.7$.[7]

Pr_2BaNiO_5. The calculation results in the ground quasidoublet for the Pr^{3+} ion with the zero-field splitting (ZFS) $\delta=32$ cm^{-1} in excellent agreement with the neutron scattering data;[6] other CF sublevels of the $^3H_4$ multiplet have energies higher than 170 cm^{-1}. Theory predicts correctly the direction of the magnetic moment (along the c axis) in the ground state. With the calculated value of the g factor $g_z=5.6$ and the measured magnetic moments $m_{z\mathrm{Pr}}=1.3$ and $m_{\mathrm{Ni}}=1.1$ at the temperature 1.5 K,[7] we obtain from Eq. (4) the molecular-field constant $\lambda=3.25T/\mu_B$, in comparison with the value $4.4T/\mu_B$ found from the magnetic susceptibility data.[12]

Tb_2BaNiO_5. The lowest fragment of the energy spectrum in the region 0–70 cm^{-1} contains six singlets; other CF sublevels of the ground multiplet $^7F_6$ have energies higher than 160 cm^{-1}. The induced magnetic moment of the Tb^{3+} ion can involve a large component along the c axis due to mixing of the ground singlet with the first excited one ($\delta=8$ cm^{-1}, $g_z/2=7.5$) and an essentially smaller component along the a axis due to mixing with the next excited singlet ($\delta=31$ cm^{-1}, $g_x/2=4.9$). These results agree with the measured magnetic moment of the Tb^{3+} ion at 1.5 K, $m_x=0.68$, and $m_z=8.0$.[7]

Ho_2BaNiO_5. Theory predicts the ground quasidoublet for the Ho^{3+} ion with a very small ZFS $\delta=0.1$ cm^{-1}; the next sublevel of the $^5I_8$ multiplet is about 80 cm^{-1} higher. The calculated magnetic moment in the ground state $g_z/2=9.4$ agrees well with the measured magnetic moment at 1.5 K, $m_x=0.12$, and $m_z=9.06$.[7] A small component of the ordered moment along the a axis can be induced by the exchange field due to mixing of the lowest singlet with the excited third singlet (the corresponding g factor equals $g_{x1,3}/2=g_J|\langle 1|J_x|3\rangle|=1.1$).

Tm_2BaNiO_5. In distinction from other rare-earth nickelates, the ordered magnetic moment of the Tm^{3+} ion has the largest component along the b axis [$m_x=-0.6$, $m_y=3.24$, and $m_z=-0.5$ at 1.5 K (Ref. 7)]. According to calculations, the CF sublevels of the ground multiplet $^3H_6$ are divided into two groups with a gap more than 250 cm^{-1}. The lowest six singlets have energies in the range 0–65 cm^{-1}. The ground state may be considered as a triplet with the zero-field splittings $\delta_{1,2}=2.4$ cm^{-1} and $\delta_{1,3}=15$ cm^{-1}. The corresponding g factors equal $g_{x1,2}=6.1$, $g_{y1,3}/2=1.6$, and $g_{z2,3}/2=3.1$. So these factors may appear compatibile with the experimental data if the exchange at the transition 1–3 is essentially stronger than at the transitions 1–2 and 2–3.

IV. SUMMARY

We have measured high-resolution (0.2 cm^{-1}) temperature-dependent (2.5–300 K) spectra of Nd^{3+} in the quantum antiferromagnet Nd_2BaNiO_5 ($T_N=47.5\pm1$ K). The diluted paramagnetic Y_2BaNiO_5:Nd(5%) compound was also studied for a comparison. The CF levels of Nd^{3+} in Nd_2BaNiO_5 found from these spectra are satisfactorily described by nine CF parameters determined from the calculations, which started with the analysis in the framework of the exchange-charge model. The Nd ground-state magnetic moments calculated using the obtained wave functions agree with those measured by the neutron diffraction method and evidence a decisive role of the Nd^{3+} single-ion anisotropy in stipulating the directions of the ordered magnetic moments in Nd_2BaNiO_5. A further successful check of the performed CF analysis consisted of a comparison between the calculated and experimental (known from the literature) energies of low-lying CF levels and low-temperature magnetic properties for the other rare-earth chain nickelates.

Our spectroscopic results on the Nd^{3+} ground-state exchange splitting $\Delta(T)$ in Nd_2BaNiO_5 unambiguously show that (i) it can be considered to occur in the effective field created by the Ni magnetic subsystem, (ii) the low-temperature behavior of the neodymium magnetic moment is determined by the $\Delta(T)$ dependence, (iii) the maximum in the temperature dependence of the magnetic susceptibility is due to depopulation of the upper component of the ground Kramers doublet split by Nd-Ni interactions, and (iv) the

4-meV mode observed in neutron scattering experiments corresponds to a flipping of a single Nd^{3+} magnetic moment.

Thus, our present study delivers information on the electronic states of Nd^{3+} in Nd_2BaNiO_5 necessary for the interpretation of previously published neutron scattering and magnetic measurements and, being combined with our earlier results on Er^{3+} in Er_2BaNiO_5, reveals a comprehensive description of CF effects in the whole series of R_2BaNiO_5 model chain nickelates.

ACKNOWLEDGMENTS

This study was supported in part by the Russian Foundation for Basic Research, Grant No. 04-02-17346, by the Russian Academy of Sciences under the Programs for Basic Research, by the Russian Ministry of Science and Technology, and by the joint CNRS-RAS program under the project No. 12234. B.Z.M. acknowledges the INTAS for support (Project No. 03-51-4943).

*Corresponding author. Electronic address: popova@isan.troitsk.ru

[1] F. D. M. Haldane, Phys. Rev. Lett. **50**, 1153 (1983).
[2] E. García-Matres, J. L. Martínez, and J. Rodríguez-Carvajal, J. Solid State Chem. **103**, 322 (1993).
[3] K. Kojima, A. Keren, L. P. Le, G. M. Luke, B. Nachumi, W. D. Wu, Y. J. Uemura, K. Kiyono, S. Miyasaka, H. Takagi, and S. Uchida, Phys. Rev. Lett. **74**, 3471 (1995).
[4] J. Darriet and L. P. Regnault, Solid State Commun. **86**, 409 (1993).
[5] G. G. Chepurko, Z. A. Kazei, D. A. Kudrjavtsev, R. Z. Levitin, B. V. Mill, M. N. Popova, and V. V. Snegirev, Phys. Lett. A **157**, 81 (1991).
[6] A. Zheludev, J. M. Tranquada, T. Vogt, and D. J. Buttrey, Phys. Rev. B **54**, 6437 (1996).
[7] E. García-Matres, J. L. Martínez, and J. Rodríguez-Carvajal, Eur. Phys. J. B **24**, 59 (2001).
[8] A. Zheludev, Physica B **241–243**, 495 (1998).
[9] T. Yokoo, A. Zheludev, M. Nakamura, and J. Akimitsu, Phys. Rev. B **55**, 11 516 (1997).
[10] T. Yokoo, S. A. Raymond, A. Zheludev, S. Maslov, E. Ressouche, I. Zaliznyak, R. Erwin, M. Nakamura, and J. Akimitsu, Phys. Rev. B **58**, 14 424 (1998).
[11] A. Zheludev, S. Maslov, T. Yokoo, J. Akimitsu, S. Raymond, S. E. Nagler, and K. Hirota, Phys. Rev. B **61**, 11 601 (2000).
[12] E. García-Matres, J. L. García-Munos, J. L. Martínez, and J. Rodríguez-Carvajal, J. Magn. Magn. Mater. **149**, 363 (1995).
[13] M. N. Popova, S. A. Klimin, E. P. Chukalina, B. Z. Malkin, R. Z. Levitin, B. V. Mill, and E. Antic-Fidancev, Phys. Rev. B **68**, 155103 (2003).
[14] G. H. Dieke, in *Spectra and Energy Levels of Rare Earth Ions in Crystals* (Interscience, New York, 1968), p. 142.
[15] P. Caro, O. Beaury, and E. Antic, J. Phys. (Paris) **37**, 671 (1976).
[16] P. Caro, E. Antic, L. Beaury, O. Beaury, J. Derouet, M. Faucher, C. Guttel, O. K. Moune, and P. Porcher (unpublished).
[17] E. Antic-Fidancev, M. Lemaitre-Blaise, and P. Caro, New J. Chem. **11**, 467 (1987).
[18] B. Z. Malkin, in *Spectroscopy of Solids Containing Rare Earth Ions*, edited by A. A. Kaplyanskii and R. M. Macfarlane (North-Holland, Amsterdam, 1987), Chap. 2, pp. 13–50.
[19] D. Sengupta and J. C. Artman, Phys. Rev. B **1**, 2986 (1970).
[20] A. J. Freeman and R. E. Watson, Phys. Rev. **127**, 2058 (1962).
[21] E. Clementi and C. Roetti, At. Data Nucl. Data Tables **14**, 177 (1974).
[22] Ch. Görller-Walrand and K. Binnemans, in *Handbook on Physics and Chemistry of Rare Earths*, edited by K. A. Gschneidner and L. Eyring (North-Holland, Amsterdam, 1996), Vol. 23, pp. 121–283.
[23] C. Boyer-Candalen, J. Derouet, P. Porcher, Y. Moelo, and A. Meerschaut, J. Solid State Chem. **165**, 228 (2002).
[24] M. N. Popova, Proc. SPIE **2706**, 182 (1996).
[25] M. N. Popova, J. Alloys Compd. **275–277**, 142 (1998).
[26] A. Zheludev, J. M. Tranquada, T. Vogt, and D. J. Buttrey, Phys. Rev. B **54**, 7210 (1996).